Nifuroxazide Suppresses PD-L1 Expression and Enhances the Efficacy of Radiotherapy in Hepatocellular Carcinoma

Abbreviated Title: Nifuroxazide prompts anti-tumor efficacy of RT

Author Names and Affiliations: Tiesuo Zhao[1,2,3], Pengkun Wei[1,2,4], Congli Zhang[1,2], Shijie Zhou[1,2], Lirui Liang[1,2,], Shuoshuo Guo[1,2], Zhinan Yin[5], Sichang Cheng[1,2], Zerui Gan[1,2], Yuanling Xia[1,2], Yongxi Zhang[6], Sheng Guo[1,2], Jiateng Zhong[2], Zishan Yang[1,2], Fei Tu[2], Qianqing Wang[7,8], Jin Bai[7,8], Feng Ren[3*], Zhiwei Feng[1,2*], Huijie Jia[2*]

[1]Department of Immunology, School of Basic Medical Sciences, Xinxiang Medical University, Xinxiang, Henan 453000, P.R.China.

[2]Xinxiang Engineering Technology Research Center of immune checkpoint drug for Liver-Intestinal Tumors, Xinxiang Medical University, Xinxiang, Henan 453000, P.R.China.

[3]Henan International Joint Laboratory of Immunity and Targeted Therapy for Liver-Intestinal Tumors, Xinxiang Medical University, Xinxiang, Henan 453000, P.R.China.

[4]Zhengzhou Central Hospital Affiliated to Zhengzhou University, Zhengzhou 450000, P.R.China.

[5]The Biomedical Translational Research Institute, Faculty of Medical Science, Jinan University, Guangzhou, China

[6]Department of Oncology, The Third Affiliated Hospital of Xinxiang Medical University, Xinxiang, Henan 453000, P.R.China.

[7]Department of Gynecology, Xinxiang Central Hospital, 453000, Xinxiang, Henan, P.R.China.

[8]The fourth clinical college, Xinxiang Medical University, Xinxiang, Henan 453000, P.R.China.

Tiesuo Zhao and Pengkun Wei contributed equally to this work.

***Corresponding authors:** Huijie Jia, MD, Xinxiang Engineering Technology Research Center of immune checkpoint drug for Liver-Intestinal Tumors, Xinxiang Medical University, Xinxiang, Henan 453000, P.R.China. Tel: +86-15090358930; Fax: +86-03733831939; Email: 131010@xxmu.edu.cn;

Zhiwei Feng, MD, PhD, Xinxiang Engineering Technology Research Center of immune checkpoint drug for Liver-Intestinal Tumors, Xinxiang Medical University, Xinxiang, Henan 453000, P.R.China.

123066@xxmu.edu.cn;

Feng Ren, MD, Henan International Joint Laboratory of Immunity and Targeted Therapy for 1`Liver-Intestinal Tumors, Xinxiang Medical University, Xinxiang, Henan 453000, P.R.China. Email: renfeng@xxmu.edu.cn

Number of pages: 26

Number of figures: 12 (+ 3 supplemental figure)

Abstract

Radiation therapy is a primary treatment for hepatocellular carcinoma (HCC), but its effectiveness can be diminished by various factors. The over-expression of PD-L1 has been identified as a critical reason for radiotherapy resistance. Previous studies have demonstrated that nifuroxazide exerts antitumor activity by damaging the Stat3 pathway, but its efficacy against PD-L1 has remained unclear. In this study, we investigated whether nifuroxazide could enhance the efficacy of radiotherapy in HCC by reducing PD-L1 expression. Our results showed that nifuroxazide significantly increased the sensitivity of tumor cells to radiation therapy by inhibiting cell proliferation and migration while increasing apoptosis *in vitro*. Additionally, nifuroxazide attenuated the up-regulation of PD-L1 expression induced by irradiation, which may be associated with increased degradation of PD-L1 through the ubiquitination-proteasome pathway. Furthermore, nifuroxazide greatly enhanced the efficacy of radiation therapy in H22-bearing mice by inhibiting tumor growth, improving survival, boosting the activation of T lymphocytes, and decelerating the ratios of Treg cells in spleens. Importantly, nifuroxazide limited the increased expression of PD-L1 in tumor tissues induced by radiation therapy. This study confirms, for the first time, that nifuroxazide can augment PD-L1 degradation to improve the efficacy of radiation therapy in HCC-bearing mice.

Keywords: Nifuroxazide, radiotherapy, hepatocellular carcinoma, PD-L1

Introduction

Cancer continues to be the primary cause of death and a major public health issue globally (1). Among the various types of cancer, hepatocellular carcinoma (HCC) has exhibited an increasing incidence and morbidity, and it is estimated that the number of new HCC cases will surpass one million by 2025 (2, 3). The current therapeutic options for HCC comprise surgery, targeted therapy, radiation therapy, chemotherapy, and immunotherapy, among others. Nevertheless, the majority of patients still experience an unfavorable prognosis. Consequently, the development of effective treatment strategies for HCC is a pressing and challenging issue (4).

Radiation therapy is a widely used localized therapeutic approach for the treatment of HCC (5, 6). It has been demonstrated that radiation therapy can induce DNA damage and mutations in tumor cells through the generation of X-rays or γ-rays, leading to the death of malignant cells (7). Despite significant progress in recent decades, the effectiveness of radiation therapy is limited by various factors. Studies have shown that radiation therapy can contribute to the formation of an immunosuppressive tumor microenvironment (TME) by promoting the infiltration of M2 macrophages, increasing the number of regulatory T cells, impairing the function of CD8+ T lymphocytes, and inducing the release of immunosuppressive cytokines (8). Therefore, improving the immunosuppressive state of HCC may enhance the clinical efficacy of radiation therapy.

Programmed cell death 1 ligand 1 (PD-L1) is a transmembrane glycoprotein predominantly expressed on T lymphocytes, B lymphocytes, macrophages, and tumor cells. Upon binding with programmed cell death protein 1 (PD-1), PD-L1 generates inhibitory signals that suppress the proliferation of T lymphocytes and accumulation of antigen-specific T cells in lymph nodes (9-11). Radiation therapy induces DNA damage and repair, activating and up-regulating PD-L1, and creating an immune-suppressive microenvironment, which is a major contributor to radiotherapy resistance of tumors (12, 13). Furthermore, tumor-associated macrophages (TAMs) also take part in shaping the tumor microenvironment by expressing PD-L1. In mice with tumors, inhibition of the PD-1/PD-L1 pathway significantly stimulated the activation of macrophages (14, 15). Similarly, in HCC, radiation therapy up-regulates the expression of PD-L1 via the IFN-γ-Stat3 signaling pathway (16). Therefore, blocking the PD-1/PD-L1 pathway may be an effective systemic treatment for enhancing the efficacy of radiation therapy.

The PD-1/PD-L1 pathway blockade has been shown to provide satisfactory clinical benefits for most

tumor types (17). However, the development and research of new drugs are time-consuming, costly, and uncertain (18), exploring the potential indications of old drugs has been endorsed by scholars (19). Nifuroxazide, an antidiarrheal drug, has been demonstrated to significantly inhibit the activation of Signal Transducer and Activator of Transcription 3 (Stat3) and has also exhibited effects in promoting the death of multiple myeloma cells and inhibiting tumor growth. Importantly, treatment with nifuroxazide has shown low toxicity that does not damage peripheral blood mononuclear cells (20). However, the relationship between nifuroxazide and the expression of PD-L1 remains unknown, as well as whether nifuroxazide can enhance the efficacy of radiation therapy in tumors by blocking the expression of PD-L1.

We have revealed that nifuroxazide exerts a significant effect on promoting the degradation of PD-L1 in HCC cells. Notably, administration of nifuroxazide led to a reduction in the expression of PD-L1 in mice, which in turn enhanced the sensitivity of radiation therapy in mice with HCC. This approach may offer a promising combination strategy to counteract the radio-resistance of HCC.

Results

The administration of Nifuroxazide augmented the radiosensitivity in the treatment of HCC

The study initially evaluated the impact of Nifuroxazide on HCC radiosensitivity by assessing cell proliferation, migration, and apoptosis. The CCK-8 assays showed that cell proliferation was significantly inhibited after adding Nifuroxazide for 24 hours, and the inhibitory effect was further enhanced when Nifuroxazide was added after radiotherapy (Fig 1A and Figure 1-figure supplement 1A). Interestingly, after 48 hours of radiotherapy, there was no significant inhibition of cell proliferation, but co-treatment with Nifuroxazide at concentrations of 2.5, 5, 10, 20, and 40 μg/ml resulted in evident inhibition. The combination of Nifuroxazide and radiotherapy also significantly inhibited cell proliferation, as demonstrated by cell cloning results (Fig 1B). Additionally, the wound-healing assay and transwell assay showed substantial hindrance of cell migration at both 24 and 48 hours after radiotherapy. The wound healing assay demonstrated that in comparison with the control group, the migratory ability of cells was significantly reduced after treatment for 24 hours in the Nifuroxazide alone group, the radiotherapy alone group and the combination group (Nifuroxazide plus radiotherapy, showing the most significant reduction) (Fig 1C and Figure 1-figure supplement 1B). Similarly, the inhibition of cell invasion was further enhanced when the cells were co-treated with Nifuroxazide and radiotherapy (Fig 1D). The combined treatment also resulted in a more potent pro-apoptotic effect on the cells. Fig. 1E and Figure 1-figure supplement 1C indicated that radiotherapy alone did not have a pro-apoptotic effect on HCC, but the combination of radiotherapy and Nifuroxazide at concentrations of 1.25, 2.5, and 5 μg/ml exhibited significant pro-apoptotic effects. These findings suggest that Nifuroxazide may serve as a promising candidate drug to improve the radiosensitivity of HCC treatment.

Nifuroxazide had a significant effect on the expression of proteins associated with cell proliferation and apoptosis

To investigate the underlying mechanism of Nifuroxazide's ability to enhance HCC radiosensitivity, the study analyzed the expression of proteins associated with proliferation and apoptosis in HCC cells. Activation of the oncogene Stat3, which plays a critical role in tumor development, was effectively inhibited by radiotherapy in cells. Moreover, Nifuroxazide, an inhibitor of Stat3, was able to suppress the activation of Stat3 in Hep G2 cells that had undergone radiotherapy, as demonstrated in Fig 2A. MMP2 plays an important role in cancer cell migration. The results showed that the combination

therapy showed a significant inhibiting effect on the expression of MMP2 (Fig 2B). The expressions of PCNA and Ki67, which are closely linked to cell proliferation, were reduced by radiotherapy. Furthermore, when administered in conjunction with Nifuroxazide, this inhibitory effect was even more pronounced, as depicted in Fig 2C and D. The combination therapy also suppressed the expression of cyclin D1, a protein involved in the cell cycle, as shown in Fig 2E. In addition, the study examined apoptotic proteins, as illustrated in Fig 2F-N. Caspase 3 is the primary enzyme responsible for the cleavage of cells during apoptosis. The results showed that the expression of cleaved-caspase 3 (c-caspase 3) was significantly increased at 24 or 48 hours after radiotherapy. Furthermore, the combination of radiotherapy and nifuroxazide resulted in a more pronounced upregulation of c-caspase 3, indicating a significant increase in cell apoptosis in HCC. Apoptosis can be induced through various pathways, with the mitochondrial apoptosis pathway being the most important. The results showed that the combination of radiotherapy and nifuroxazide had a significant impact on the expression of Bax, Bcl-2, and cytochrome C. Specifically, the combination therapy inhibited the expression of Bcl-2, which led to the translocation of Bax to mitochondria and the release of cytochrome C into the cytoplasm. The release of cytochrome C subsequently activated caspase 9, another pro-apoptotic protein. These events indicate that radiotherapy in combination with nifuroxazide significantly enhances apoptosis in HCC. PARP is the substrate of caspases and plays a vital role in regulating apoptosis. The activation of PARP is considered an important indicator of cell apoptosis and caspase 3 activation. The results demonstrated that the combination therapy increased the expression of c-PARP, suggesting that it had significant capabilities in inducing apoptosis. Overall, these findings suggest that the combination of radiotherapy and nifuroxazide can inhibit proliferation and increase apoptosis in HCC by regulating different tumor-related proteins.

Radiotherapy in combination with nifuroxazide significantly inhibited the growth of tumors in tumor-bearing mice and prolonged their survival period

A tumor-bearing mice model was used to validate the anti-tumor effect of the combination treatment. The treatment protocol for the study is illustrated in Fig 3A. Seven days after the final treatment, the tumors were extracted, and the size and weight of the tumors were measured. The results showed that both the radiation therapy and nifuroxazide treatment groups exhibited significant inhibition of tumor growth compared to the PBS group, as evidenced by smaller tumor size and weight. Moreover, the combination treatment group demonstrated even greater inhibition of tumor growth than either

mono-treatment group (Fig 3B and C). Notably, the combination treatment also significantly prolonged the survival of tumor-bearing mice, with three mice still surviving on the 60th day (Fig 3D). Histological analysis using HE staining showed that the tumor cells in the PBS group had irregular shape, high nucleo-cytoplasmic ratio, significant increase in heterotypic nuclei, and more pleomorphism of nuclei. However, the histomorphology significantly improved after the treatment with nifuroxazide and radiation therapy (Fig 3E). Histological analysis using HE staining showed that, in the PBS group, tumor cells exhibited vigorous growth, tight arrangement, irregular shape, high nucleo-cytoplasmic ratio, significant increase in heterotypic nuclei, and more pleomorphism of nuclei. After treatment, the tumor cell arrangement became loose, and the cells displayed an irregular shape, with large vacuoles or vacancies, as well as necrosis or ablation phenomena. These changes were most significant in the combination treatment group, suggesting that the histomorphology significantly improved after the treatment with nifuroxazide and radiation therapy (Fig 3E). These findings indicated that nifuroxazide played a crucial role in enhancing the efficacy of radiotherapy for HCC.

The combination of radiotherapy and nifuroxazide showed a remarkable inhibition of cell proliferation and an increase in cell apoptosis in tumor tissues

To further elucidate the anti-tumor mechanism of combining radiotherapy with nifuroxazide, the expression of proteins related to proliferation and apoptosis was evaluated in tumor tissues of tumor-bearing mice. As showed in Fig 4A-C, the combination therapy significantly suppressed the expression of Ki67 and PCNA in tumor tissues while promoting the activation of caspase3, indicating its efficacy in hindering tumor cell proliferation and inducing apoptosis. Additionally, the TUNEL assay showed a marked increase in the apoptotic rate of tumor cells upon the combination therapy (Fig 4D). Moreover, the levels of proteins involved in cell proliferation (p-Stat3, PCNA, Ki67, and cyclin D1) and cell migration (MMP2) were analyzed in the tumor tissues. Fig 4E-I revealed that the combination therapy strikingly reduced the levels of associated proteins, indicating its potential in suppressing tumor cell proliferation. Subsequently, the cell apoptosis in tumor tissues was evaluated, and the expression of pro-apoptotic proteins (c-caspase3, Bax, and Cytochrome C) was observed to be significantly upregulated in the tumor tissues of mice treated with radiotherapy plus nifuroxazide, whereas the expression of anti-apoptotic protein (BCL-2) was downregulated (Fig 4J-N). These results suggest that the combination therapy of radiotherapy and nifuroxazide effectively inhibits tumor cell proliferation and induces apoptosis by regulating the expression of proteins related to proliferation and

apoptosis.

The combination of radiotherapy and nifuroxazide significantly boosted the activation of tumor-infiltrating lymphocytes and increased the population of M1 macrophages in tumor bearing mice

The impact of combining radiotherapy with nifuroxazide was comprehensively elucidated by assessing the infiltration of lymphocytes and M1 macrophages in tumor tissues. The combination therapy significantly augmented the infiltration of $CD4^+$ (Fig 5A, 5E and Figure 5-figure supplement 2A, confirmed by both immunofluorescence and flow cytometry) and $CD8^+$ (Fig 5B, 5E and Figure 5-figure supplement 2B, confirmed by both immunofluorescence and flow cytometry) lymphocytes, and stimulated the activation of lymphocytes (Granzyme B^+) (Fig 5C, 5E and Figure 5-figure supplement 2C, confirmed by both immunofluorescence and flow cytometry). Additionally, it increased the polarization of M1 macrophages ($CD11^+$ $CD86^+$) (Fig 5D and 5E). Moreover, the combination therapy increased the infiltration of NK cells (Figure 5-figure supplement 2D) and decreased the number of Treg cells (Figure 5-figure supplement 2E) in the cancer tissues of the HCC-bearing mice. Furthermore, the expression of associated proteins also demonstrated the same results (Fig 5F-I). These findings indicate that the combination of radiotherapy and nifuroxazide can effectively enhance the anti-tumor immune response in mice with tumors.

Radiotherapy combined with nifuroxazide noticeably regulated the ratios of immune cells in the spleens

As the spleen is an essential immune organ, it plays a crucial role in the peripheral immune response. To quantify the ratios of immune cells in different groups of tumor-bearing mice, flow cytometry was employed. The results showed that treatment with radiotherapy or nifuroxazide led to a substantial increase in the number of $CD8^+$ lymphocytes, activated lymphocytes (Granzyme B^+), M1 macrophages and NK cells in the spleens of mice compared to the PBS group. Moreover, the combined treatment resulted in the highest number of these cells among all the groups (Fig 6B, D, E and F). Additionally, the ratio of $CD4^+$ T lymphocytes in the spleens of mice treated with radiotherapy did not show any difference when compared to the PBS group. However, the ratio was significantly increased when radiotherapy was combined with nifuroxazide (Fig 6A). Furthermore, Treg cells are crucial immunosuppressive cells that facilitate the immune evasion of tumor cells. Our findings indicate that treatment with radiotherapy leads to a significant increase in the ratio of Treg cells (Fig 6C). However,

the trend could be reversed after administering nifuroxazide treatment, suggesting that nifuroxazide may enhance the antitumor effects of radiotherapy by regulating the immune response.

Nifuroxazide in combination with the radiotherapy significantly increased the degradation of PD-L1 through ubiquitin-proteasome pathway

PD-L1 is a co-inhibitory protein expressed by various cells, including tumor cells, and its pathway has been shown to inhibit the anti-tumor function of T lymphocytes. PD-L1 is considered a critical indicator of radiotherapy resistance. Therefore, we investigated whether nifuroxazide enhances radiosensitivity in HCC via the PD-1/PD-L1 pathway. Our results showed that radiotherapy significantly inhibited the expression of p-Stat3 (Fig 2A, B), but induced the upregulation of PD-L1 expression, which was effectively reversed by combined treatment with nifuroxazide (Fig 7A and Figure 7-figure supplement 3A, in both HepG2 and Huh7 cell lines). These results suggest that nifuroxazide may be a potential PD-L1 inhibitor, but its effect is independent of the Stat3 pathway. Surprisingly, we found that radiotherapy also upregulated PD-L1 mRNA expression, which was not affected by nifuroxazide treatment (Fig 7B and Figure 7-figure supplement 3B, in both HepG2 and Huh7 cell lines). These results suggest that nifuroxazide cannot regulate PD-L1 gene expression. The proteasome pathway is a key pathway involved in protein degradation. Our findings demonstrate that the inhibitory effect of nifuroxazide on PD-L1 expression was counteracted by the proteasome inhibitor (Fig 7C and Figure 7-figure supplement 3C, in both HepG2 and Huh7 cell lines). Moreover, nifuroxazide treatment clearly increased the expression of GSK3β (Fig 7D). Additionally, the inhibitor of GSK3β reversed the downregulation of *CD274* expression in cells treated with nifuroxazide (Fig 7E). These findings confirmed that nifuroxazide could increase the degradation of PD-L1 via the ubiquitin-proteasome pathway and ultimately restore the immunity of T lymphocytes (Fig 7F).

The combination of Nifuroxazide and radiotherapy notably inhibited the expression of PD-L1 via the up-regulation of GSK3β expression

We next detected the expression level of PD-L1 in tumor tissues of HCC patients pre-and post-radiotherapy. The results showed a significant increase in PD-L1 expression in tumor tissues of HCC patients after radiotherapy, compared to pre-radiotherapy (Fig 8A), which may account for the poor clinical response to radiotherapy. Similarly, we observed an elevation in PD-L1 expression in tumor tissues of mice receiving radiotherapy. However, treatment with Nifuroxazide effectively blocked the up-regulation of PD-L1 induced by radiotherapy (Fig 8B and C). Notably, the study

demonstrated that treatment with Nifuroxazide significantly increased the expression of GSK3β in mice, regardless of radiotherapy treatment (Fig 8D). These findings suggest that Nifuroxazide may enhance the degradation of PD-L1 and improve the therapeutic response to radiotherapy.

Discussion

Radiation therapy is a crucial approach in the management of HCC, but its effectiveness is limited by radioresistance. Our investigation has confirmed that nifuroxazide can enhance the immune response against tumors induced by radiation therapy by promoting the degradation of PD-L1 in HCC. PD-L1 is predominantly expressed on the surface of tumor cells and severely obstructs the immune response against tumors by binding to PD-1. Several studies have indicated that overexpression of PD-L1 is a major cause of radioresistance (21-23). Therefore, inhibition of PD-L1 may prove to be an effective strategy to strengthen the antitumor effect of radiation therapy. D-mannose has been reported to significantly enhance the effects of radiotherapy by promoting PD-L1 degradation in triple-negative breast tumors (24). Additionally, Stat3 plays a key role in tumor progression and also regulates PD-L1 expression (25). Therefore, investigating Stat3 inhibitors could offer a fresh perspective on suppressing PD-L1 expression. A new Stat3 inhibitor was discovered, which is nifuroxazide, previously used to treat diarrhea (20). Our study showed that nifuroxazide significantly inhibited the protein expression of PD-L1. Further investigations demonstrated that radiation therapy upregulated the gene level of PD-L1, while nifuroxazide did not change the gene level *in vitro*. Intriguingly, nifuroxazide covertly promoted the expression of GSK3β in cells that have undergone radiography. Simultaneously, the protease inhibitor blocked the inhibitory effect on PD-L1 expression. This finding suggests that nifuroxazide modulates the PD-L1 pathway through the ubiquitin-proteasome pathway rather than the mRNA pathway.

The anti-tumor role of nifuroxazide has been reported. However, the innovation of our study does not lie in confirming its antitumor effects but rather in demonstrating how nifuroxazide can enhance radiotherapy's efficacy in treating hepatocellular carcinoma by inhibiting PD-L1 levels. We compared the efficacy of the combination therapy versus radiotherapy and found that compared to radiotherapy alone, the combination therapy more significantly inhibited hepatocellular carcinoma cell proliferation and migration. In our animal model, we compared the therapeutic effects of the combination therapy, nifuroxazide alone, and radiotherapy alone on hepatocellular carcinoma-bearing mice. We observed that compared to individual treatment groups, the combination therapy more profoundly suppressed tumor growth and enhanced the antitumor effects in the mice.

The primary objective of this study is to explore whether nifuroxazide can effectively enhance the degradation of PD-L1, thereby increasing the radiosensitivity of HCC. Our research reveals that

compared to radiation therapy alone, combination therapy involving nifuroxazide and radiation significantly inhibits tumor growth in mice and boosts the anti-tumor immune response. This finding could potentially provide a valuable strategy for patients who exhibit resistance to radiation therapy in clinical practice. Moreover, clinical trial investigations have demonstrated that nivolumab, a PD-1 monoclonal antibody, when combined with radiotherapy for HCC, exhibits promising safety and efficacy (26). This evidence supports the future application of nifuroxazide in the treatment of HCC. However, to reach this objective, we must continue to conduct extensive research, including comparing nifuroxazide with existing therapies in clinical practice. In this study, nifuroxazide not only significantly inhibits the expression of PD-L1 protein in HCC cells but also functions as a PD-L1 inhibitor. Furthermore, it effectively curbs the proliferation and migration of HCC cells, induces tumor cell apoptosis, and may exhibit enhanced anti-tumor effects, making it a promising candidate for clinical use. We believe that the advantage of nifuroxazide over PD-1 or PD-L1 antibodies lies in its ability not only to effectively inhibit PD-L1 expression but also to suppress tumor cell proliferation, migration, and promote tumor cell apoptosis.

We analyzed the underlying anti-tumor mechanism of nifuroxazide in terms of cell proliferation, migration and drug action target. Research has shown that regulating the STAT3/PD-L1 pathway can effectively increase apoptosis in lung cancer cells (27). Our study confirmed that nifuroxazide can effectively inhibit the expression of p-STAT3 and PD-L1 in liver cancer cells, which may be the reason for the increased apoptosis of these cells. Nifuroxazide has been demonstrated to inhibit the expression of p-STAT3, thereby suppressing tumor cell proliferation and migration (20, 28). In our study, we observed that after 48 hours of treatment with nifuroxazide, the expression of p-STAT3 in irradiated cells was significantly inhibited. Furthermore, compared to radiotherapy alone, combining nifuroxazide and radiotherapy resulted in a more pronounced decrease in PCNA expression. Simultaneously, we performed additional detection of migration-related protein MMP2, confirming that combining nifuroxazide and radiotherapy led to a more significant inhibition of MMP2 expression. These findings suggest that the combination treatment may be responsible for the synergistic suppression of HCC cell proliferation and migration. Our initial results indicate that nifuroxazide inhibits the expression of PD-L1 at the protein level, but does not affect its mRNA level. Interestingly, upon treatment with a proteasome inhibitor MG132, the inhibitory effect of nifuroxazide on PD-L1 was eliminated, suggesting that nifuroxazide may enhance the degradation of PD-L1 protein. Our experiments have

demonstrated the inhibitory effect of Nifuroxazide on PD-L1 in both human and mouse cell lines.

Furthermore, the overexpression expression of PD-L1 hinders the antitumor immunity response by inhibiting T lymphocyte function and macrophage polarization (29, 30). The activity of T lymphocytes is closely associated with tumor progression, but it can become dysregulated due to the interaction between PD-1 and PD-L1 (31, 32). Blocking the PD-1 and PD-L1 pathway can reverse T cell exhaustion and enhance their ability to eliminate tumor cells (33). In our study, treatment with nifuroxazide effectively boosted T cell activation, with a more pronounced effect observed in mice receiving radiation therapy. Radiation therapy has been shown to induce an immunogenic effect that promotes T lymphocyte infiltration into tumors (34), but it also induces PD-L1 expression, which impairs T lymphocyte function (35). Under these circumstances, nifuroxazide significantly enhanced T lymphocyte activation in mice receiving radiation therapy by reducing PD-L1 expression.

Moreover, the upregulation of PD-L1 on the surface of macrophages has been found to promote the reduction of M1 macrophage polarization, which is recruited by tumor cells, leading to the inhibition of antitumor immunity (14, 36). Studies have indicated a distinct decline in M1 macrophages in tumor tissues of patients undergoing radiation therapy (37, 38). Therefore, a crucial strategy to enhance the antitumor effect of radiation therapy is to reverse macrophage polarization. Our research confirmed that nifuroxazide had a positive effect on promoting M1 macrophage polarization. Notably, while radiation therapy suppressed the infiltration of M1 macrophages, the number of M1 macrophages significantly increased in tumor tissues of mice treated with nifuroxazide and radiation therapy. These findings demonstrate that nifuroxazide plays a vital role in strengthening the antitumor immunity of radiation therapy for HCC by reversing macrophage polarization.

To summarize, the antitumor effect of radiation therapy is impaired due to the induction of PD-L1 expression. High expression of PD-L1 hinders the antitumor function of T lymphocytes and macrophages. However, nifuroxazide significantly inhibits PD-L1 up-regulation induced by radiation therapy, enhances the activation of T lymphocytes and the ratio of M1 macrophages, and decreases the number of Treg cells (Fig. 9). We confirm that nifuroxazide improves the antitumor effect of radiotherapy and provides a synergistic therapeutic strategy for HCC patients, especially those who are radioresistant. However, to achieve the goal of applying nifuroxazide combined with radiation therapy for the treatment of clinical hepatocellular carcinoma, we still need to undertake extensive research, including validation on genetically identical mouse HCC tumor models.

Materials and methods

Regents and cell lines

The Nifuroxazide used in this study was obtained from Sigma-Aldrich (USA). The HepG2, Huh7 and H22 cell lines were maintained at Xinxiang Key Laboratory of Tumor Vaccine and Immunotherapy, located at Xinxiang Medical University in Xinxiang, Henan (P.R. China).

Cell viability assay

HepG2 and Huh7 cells were cultured and seeded in 96-well plates (Corning, New York, NY) at a density of 1×10^4/well. After 15 hours of incubation, nifuroxazide with varying concentrations (0, 0.3125, 0.625, 1.25, 2.5, 5, 10, 20, 40 μg/mL) were added and co-incubated for 24 or 48 hours with or without radiotherapy treatment. After the incubation period, Cell Counting Kit-8 (CCK-8, Beyotime Institute of Biotechnology, Shanghai, China) reagents were added into each well and incubated for an additional 2 hours. The optical density (OD) was measured at 450 nm using a microplate reader (SpectraMax iD3, Molecmlar Devices).

Wound-Healing assay

HepG2 and Huh7 cells were cultured and subjected to radiotherapy, then seeded in six-well plates (Corning, New York, NY) at a density of 3.5×10^5 cells per well, followed by an incubation period of 15 hours. A scratch was created in the middle of each well using a pipette tip. Afterwards, the cells were co-cultured with varying concentrations of nifuroxazide (0, 0.625, 1.25, 2.5, 5 μg/mL) for a period of 24 or 48 hours. Subsequently, the width of the scratch was recorded and measured.

Colony formation

HepG2 cells were treated with or without radiotherapy and then plated at a density of 2×10^3 cells per well in six-well plates from Corning, New York, NY. After an incubation period of 15 hours, nifuroxazide was added at various concentrations (0, 0.625, 1.25, 2.5, 5 μg/mL). The culture medium was periodically replaced and cell masses became visible by the 10th day. Subsequently, the cell colonies were detected and recorded.

Transwell

HepG2 cells were treated with or without radiotherapy and then plated at a density of 1×10^5 cells per well in the upper chamber, while different concentrations of nifuroxazide (0, 0.625, 1.25, 2.5, 5 μg/mL) were added. Meanwhile, 500 μL of culture medium was added to the lower chamber. After a 24-hour incubation period, the lower chambers were drained and stained with crystal violet for 40 minutes. The

results were subsequently observed under a microscope (Nikon, Japan) after sealing with neutral resin.

RT-PCR

HepG2 cells, treated with or without radiotherapy, were seeded at a density of 3.5×10^5 cells per well in six-well plates from Corning, New York, NY, and incubated for 15 hours. Nifuroxazide was then added at varying concentrations (0, 0.625, 1.25, 2.5, 5 μg/mL) into each well. After a period of 24 or 48 hours, total RNA was extracted from the cells using the Trizol reagent, following the instructions. The gene expression of *CD274* was subsequently detected using PCR. The PCR primers used were as follows: For GAPDH, Forward-sequence: AGAAGGCTGGGGCTCATTTG, and Reverse-sequence: AGGGGCCATCCACAGTCTTC. For PD-L1, Forward-sequence: GAGCGTGACAAGAGGAAGGAATGG, and Reverse-sequence: TTGAGGCATTGAGTGGAGGCAAAG.

Detection of mRNA levels

Calculate and perform statistical analysis on the gray values of the agarose gel electrophoresis bands. Divide the gray value of the target gene by the gray value of the internal control to correct for errors. The resulting value represents the relative content of the target gene in a specific sample.

Establishment of tumor model and therapeutic options

The female C57BL/6 mice with 6-8 weeks were procured from Skbex Biotechnology in Henan, China. The animal studies were approved by the Ethics Committee of Xinxiang Medical University located in Xinxiang, China. H22 cells were subcutaneously injected into the right dorsal of the mice at a concentration of 2×10^6/100 μl. After 7 days, the mice were randomly assigned to one of four groups: the PBS group, Radiation therapy group, nifuroxazide group, Radiation therapy plus Nifuroxazide group. Seven days after the inoculation, the mice were anesthetized using 1% sodium pentobarbital and underwent radiation therapy at a dose of 4 Gy. The following day, nifuroxazide was intratumorally injected at a dose of 200 μg per mouse once a day. On the eighth day after the last treatment, relevant indicators were measured. The number of mice for survival rate is 10 per group, while the number of mice for the other experiment is 6 per group.

Western blot

Total proteins were extracted using RIPA lysate buffer (Beyotime Institute of Biotechnology, Shanghai, China) for western blot detection. Briefly, the proteins were separated via 10% sodium dodecyl sulfate–polyacrylamide gel electrophoresis (SDS–PAGE). Following electrophoresis, the proteins were

transferred to polyvinylidene fluoride membrane (EMD Millipore, Billerica, MA, USA). The PVDF membranes were then incubated with a buffer of 5% nonfat dry milk for 2 hours at room temperature. After being washed, the membranes were incubated with the following primary antibodies overnight at 4 ℃: PD-L1 (1:1000, Bioworld), p-Stat3 (1:1000, CST), Stat3 (1:1000, Bioworld), cleaved-caspase 3 (1:1000, Bioworld), Pro-Caspase 3 (1:2000, Bioworld), MMP2 (1:1000, CST), Ki67 (1:1000, Bioworld), PCNA (1:1000, SANTA), GSK3β (1:2000, Abways), cyclin D1 (1:2000, SANTA), Bcl-2 (1:2000, Abways), Bax (1:2000, Abways), Cytochrome C (1:1000, Biopple), cleaved-caspase 9 (1:2000, Abways), Pro-Caspase 9 (1:2000, Abways), PARP (1:1000, CST), cleaved-PARP (1:1000, CST), and Tubulin (1:1000, Sigma). The membranes were then washed and incubated with secondary antibodies (ZSGB-BIO, 1:5000). Finally, specific protein bands were visible using enhanced chemiluminescence (Beyotime Institute of Biotechnology) and detected using the chemiluminescence imaging instrument (Fusion FX spectra, Vilber). The images were semi-quantified using Quantity One software (Version 4.62; Bio-Rad Laboratories, Inc., Hercules, CA, USA).

Hematoxylin and eosin (HE) staining

Tumor tissue waxes were utilized to prepare tissue sections with a thickness of 4 μm. Following dewaxing and dehydration, the sections were stained using haematoxylin-eosin (Beyotime Biotechnology, Shanghai, China). Subsequently, the sections were rinsed and dried, and the resulting images were observed utilizing a microscope (Nikon, Japan). The tumor tissue is graded according to histological standards, including assessment of irregular tumor cell nuclei, nuclear abnormalities, and nuclear-to-cytoplasmic ratio. The scoring system for abnormal nuclei and nuclear-to-cytoplasmic ratio is as follows: 10% to 20% = 1 point, 20% to 30% = 2 points, and greater than 30% = 3 points.

Immunohistochemistry (IHC)

Following preparation as previously described (39), the tissue sections were incubated with primary antibodies against Ki67 and cleaved-caspase3, both purchased from Cell Signaling Technology (USA), overnight at 4 ℃. Subsequently, the sections were washed and incubated with biotin-labeled secondary antibodies for 30 minutes. After the completion of the reaction, streptavidin labeled with horseradish peroxidase was added. After a 30-minute incubation, the sections were chromogenically stained using the DAB reagent. Finally, the results were recorded utilizing a digital scanner (3DHISTECH, Pannoramic MIDI, China).

Immunofluorescence (IF)

The tissue samples were incubated with primary antibodies (CD3, 1:100, OmnimAbs; CD4, 1:200, CST; CD8, 1:800, CST; Granzyme B, 1:200, Bioworld; CD86, 1:400, Novus; CD11b, 1:200, Abways; PD-L1, 1:200, Bioworld) overnight at 4 ℃. Subsequently, the samples were rinsed and exposed to secondary antibodies labeled with corresponding fluorescent markers (Abways). After incubating at room temperature for 30 minutes, the samples were stained with DAPI solution (Beyotime) and incubated for 5 minutes at room temperature. Lastly, the samples were washed and sealed with anti-fluorescence quenching agent, and the images were captured using a confocal microscope (AR1+, Nikon).

TUNEL

The detection of cell apoptosis in tumor tissues was conducted via TUNEL assay in accordance with the instructions provided in the manual from Beyotime Biotechnology. In brief, tumor sections were exposed to TUNEL detection solution and incubated at 37 ℃ for 60 minutes. Following a wash step, the sections were incubated with an anti-fluorescence quenching agent. The resulting images were captured using a confocal microscope (AR1+, Nikon).

Flow Cytometry

Spleen cell suspensions were prepared and the removal of red blood cells was accomplished with the use of erythrocyte lysate solution (Beyotime Biotechnology). The concentration of cells was then adjusted to 1×10^7 cells/ml. Subsequently, 100 μL of cell suspension was separately incubated with CD3, CD4, CD8, CD25, Foxp3, NK1.1, CD86, F4/80 and Granzyme B antibodies (Biolegend) for 30 minutes. The cells were then washed using PBS buffer, and the ratios of immune cells were assessed utilizing flow cytometry (Cyto FLEX, Beckman).

Statistical analysis

Measurement data are expressed as the mean ± SD of three independent experiments, obtained from three separate and independent experimental trials. Statistical analysis was conducted using SPSS version 19.0, developed by IBM Corporation. Multigroup comparisons of the means were carried out by one-way analysis of variance (ANOVA) test with post hoc contrasts by Student–Newman–Keuls test, and the survival rate was analyzed using the Kaplan-Meier method with a log-rank test. Results with *P*-values below 0.05 were deemed to be statistically significant.

Acknowledgements

This study was financially supported by the Doctor Launch Fund of Xinxiang Medical University (grant nos. 505017, 502006 and 505016), and the Key Projects of Scientific Research for Higher Education of Henan Province (grant no. 21A310012), the Young Backbone Teacher Training Projects of Universities in Henan province (grant no. 2020GGJS149), the Science and Technology Research Project of Henan Province (grant no. 222102310016), the Major Science and Technology Project of Xinxiang City (ZD2020005), the Science and Technology Project of Xinxiang (GG2019043), the Medical Education Research Project of Henan Province (grant no. Wjlx2020305), the Teaching and Scientific Research Program of Basic Medical College, Xinxiang Medical University (grant no. JCYXYJX202006), the Graduate Student Innovation Support Plan (grant no. YJSCX202149Y), the Innovation and Entrepreneurship Training Programmed for college student (grant no. 202210472005), Key Research and Development Projects in Henan Province (grant no. 231111311300).

Conflict of interest statement:

The authors declare no competing financial interests.

Ethics statement

This study was performed in accordance with the national guidelines, and with the approval of the institution for the care and use of animals (IACUC) and Ethics Committee of Xinxiang Medical University (Xinxiang, China).

Data Availability Statement

Data that supports these findings are available from the corresponding authors upon reasonable request.

REFERENCES

1. Siegel RL, Miller KD, Fuchs HE, Jemal A. Cancer Statistics, 2021. CA Cancer J Clin. 2021;71(1):7-33. doi: 10.3322/caac.21654.
2. Feng RM, Zong YN, Cao SM, Xu RH. Current cancer situation in China: good or bad news from the 2018 Global Cancer Statistics? Cancer Commun (Lond). 2019;39(1):22. doi: 10.1186/s40880-019-0368-6.
3. Hepatocellular carcinoma. Nat Rev Dis Primers. 2021;7(1):7. doi: 10.1038/s41572-021-00245-6.
4. Jiri T, Igor K, Mba. Hepatocellular carcinoma future treatment options. Klin Onkol. 2020;33(Supplementum 3):26-9. doi: 10.14735/amko20203S26.
5. Klein J, Dawson LA. Hepatocellular carcinoma radiation therapy: review of evidence and future opportunities. Int J Radiat Oncol Biol Phys. 2013;87(1):22-32. doi: 10.1016/j.ijrobp.2012.08.043.
6. Chen B, Wu JX, Cheng SH, Wang LM, Rong WQ, Wu F, et al. Phase 2 Study of Adjuvant Radiotherapy Following Narrow-Margin Hepatectomy in Patients With HCC. Hepatology. 2021;74(5):2595-604. doi: 10.1002/hep.31993.
7. Barber GN. STING: infection, inflammation and cancer. Nature reviews Immunology. 2015;15(12):760-70. doi: 10.1038/nri3921.
8. Shevtsov M, Sato H, Multhoff G, Shibata A. Novel Approaches to Improve the Efficacy of Immuno-Radiotherapy. Front Oncol. 2019;9:156. doi: 10.3389/fonc.2019.00156.
9. Sato H, Okonogi N, Nakano T. Rationale of combination of anti-PD-1/PD-L1 antibody therapy and radiotherapy for cancer treatment. Int J Clin Oncol. 2020;25(5):801-9. doi: 10.1007/s10147-020-01666-1.
10. Voli F, Valli E, Lerra L, Kimpton K, Saletta F, Giorgi FM, et al. Intratumoral Copper Modulates PD-L1 Expression and Influences Tumor Immune Evasion. Cancer research. 2020;80(19):4129-44. doi: 10.1158/0008-5472.CAN-20-0471.
11. Wang X, Yang X, Zhang C, Wang Y, Cheng T, Duan L, et al. Tumor cell-intrinsic PD-1 receptor is a tumor suppressor and mediates resistance to PD-1 blockade therapy. Proc Natl Acad Sci U S A. 2020;117(12):6640-50. doi: 10.1073/pnas.1921445117.
12. Azad A, Yin Lim S, D'Costa Z, Jones K, Diana A, Sansom OJ, et al. PD-L1 blockade enhances response of pancreatic ductal adenocarcinoma to radiotherapy. EMBO Mol Med. 2017;9(2):167-80. doi: 10.15252/emmm.201606674.

13. Gong X, Li X, Jiang T, Xie H, Zhu Z, Zhou F, et al. Combined Radiotherapy and Anti-PD-L1 Antibody Synergistically Enhances Antitumor Effect in Non-Small Cell Lung Cancer. J Thorac Oncol. 2017;12(7):1085-97. doi: 10.1016/j.jtho.2017.04.014.

14. Hartley GP, Chow L, Ammons DT, Wheat WH, Dow SW. Programmed Cell Death Ligand 1 (PD-L1) Signaling Regulates Macrophage Proliferation and Activation. Cancer Immunol Res. 2018;6(10):1260-73. doi: 10.1158/2326-6066.CIR-17-0537.

15. Sumitomo R, Hirai T, Fujita M, Murakami H, Otake Y, Huang CL. PD-L1 expression on tumor-infiltrating immune cells is highly associated with M2 TAM and aggressive malignant potential in patients with resected non-small cell lung cancer. Lung Cancer. 2019;136:136-44. doi: 10.1016/j.lungcan.2019.08.023.

16. Greten TF, Sangro B. Targets for immunotherapy of liver cancer. J Hepatol. 2017. doi: 10.1016/j.jhep.2017.09.007.

17. Salmaninejad A, Valilou SF, Shabgah AG, Aslani S, Alimardani M, Pasdar A, et al. PD-1/PD-L1 pathway: Basic biology and role in cancer immunotherapy. J Cell Physiol. 2019;234(10):16824-37. doi: 10.1002/jcp.28358.

18. Scannell JW, Blanckley A, Boldon H, Warrington B. Diagnosing the decline in pharmaceutical R&D efficiency. Nat Rev Drug Discov. 2012;11(3):191-200. doi: 10.1038/nrd3681.

19. Wu E. discovering new anticancer activities from old drugs. Curr Med Chem. 2013;20(33):4093-4. doi: 10.2174/09298673113209990193.

20. Nelson EA, Walker SR, Kepich A, Gashin LB, Hideshima T, Ikeda H, et al. Nifuroxazide inhibits survival of multiple myeloma cells by directly inhibiting STAT3. Blood. 2008;112(13):5095-102. doi: 10.1182/blood-2007-12-129718.

21. Boustani J, Lecoester B, Baude J, Latour C, Adotevi O, Mirjolet C, et al. Anti-PD-1/Anti-PD-L1 Drugs and Radiation Therapy: Combinations and Optimization Strategies. Cancers. 2021;13(19). doi: 10.3390/cancers13194893.

22. Yi M, Zheng X, Niu M, Zhu S, Ge H, Wu K. Combination strategies with PD-1/PD-L1 blockade: current advances and future directions. Mol Cancer. 2022;21(1):28. doi: 10.1186/s12943-021-01489-2.

23. Gong J, Le TQ, Massarelli E, Hendifar AE, Tuli R. Radiation therapy and PD-1/PD-L1 blockade: the clinical development of an evolving anticancer combination. J Immunother Cancer. 2018;6(1):46. doi: 10.1186/s40425-018-0361-7.

24. Zhang R, Yang Y, Dong W, Lin M, He J, Zhang X, et al. D-mannose facilitates immunotherapy and radiotherapy of triple-negative breast cancer via degradation of PD-L1. Proc Natl Acad Sci U S A. 2022;119(8). doi: 10.1073/pnas.2114851119.

25. Tong L, Li J, Li Q, Wang X, Medikonda R, Zhao T, et al. ACT001 reduces the expression of PD-L1 by inhibiting the phosphorylation of STAT3 in glioblastoma. Theranostics. 2020;10(13):5943-56. doi: 10.7150/thno.41498.

26. de la Torre-Alaez M, Matilla A, Varela M, Inarrairaegui M, Reig M, Lledo JL, et al. Nivolumab after selective internal radiation therapy for the treatment of hepatocellular carcinoma: a phase 2, single-arm study. Journal for immunotherapy of cancer. 2022;10(11). doi: 10.1136/jitc-2022-005457.

27. Xie C, Zhou X, Liang C, Li X, Ge M, Chen Y, et al. Apatinib triggers autophagic and apoptotic cell death via VEGFR2/STAT3/PD-L1 and ROS/Nrf2/p62 signaling in lung cancer. Journal of experimental & clinical cancer research : CR. 2021;40(1):266. doi: 10.1186/s13046-021-02069-4.

28. Yang F, Hu M, Lei Q, Xia Y, Zhu Y, Song X, et al. Nifuroxazide induces apoptosis and impairs pulmonary metastasis in breast cancer model. Cell Death Dis. 2015;6(3):e1701. doi: 10.1038/cddis.2015.63.

29. Cousin N, Cap S, Dihr M, Tacconi C, Detmar M, Dieterich LC. Lymphatic PD-L1 Expression Restricts Tumor-Specific CD8(+) T-cell Responses. Cancer Res. 2021;81(15):4133-44. doi: 10.1158/0008-5472.CAN-21-0633.

30. Xiong H, Mittman S, Rodriguez R, Moskalenko M, Pacheco-Sanchez P, Yang Y, et al. Anti-PD-L1 Treatment Results in Functional Remodeling of the Macrophage Compartment. Cancer research. 2019;79(7):1493-506. doi: 10.1158/0008-5472.CAN-18-3208.

31. Sun C, Mezzadra R, Schumacher TN. Regulation and Function of the PD-L1 Checkpoint. Immunity. 2018;48(3):434-52. doi: 10.1016/j.immuni.2018.03.014.

32. Dammeijer F, van Gulijk M, Mulder EE, Lukkes M, Klaase L, van den Bosch T, et al. The PD-1/PD-L1-Checkpoint Restrains T cell Immunity in Tumor-Draining Lymph Nodes. Cancer cell. 2020;38(5):685-700 e8. doi: 10.1016/j.ccell.2020.09.001.

33. Budimir N, Thomas GD, Dolina JS, Salek-Ardakani S. Reversing T-cell Exhaustion in Cancer: Lessons Learned from PD-1/PD-L1 Immune Checkpoint Blockade. Cancer Immunol Res. 2022;10(2):146-53. doi: 10.1158/2326-6066.CIR-21-0515.

34. Lhuillier C, Rudqvist NP, Elemento O, Formenti SC, Demaria S. Radiation therapy and

anti-tumor immunity: exposing immunogenic mutations to the immune system. Genome Med. 2019;11(1):40. doi: 10.1186/s13073-019-0653-7.

35. Lan Y, Moustafa M, Knoll M, Xu C, Furkel J, Lazorchak A, et al. Simultaneous targeting of TGF-beta/PD-L1 synergizes with radiotherapy by reprogramming the tumor microenvironment to overcome immune evasion. Cancer Cell. 2021;39(10):1388-403 e10. doi: 10.1016/j.ccell.2021.08.008.

36. Ubil E, Caskey L, Holtzhausen A, Hunter D, Story C, Earp HS. Tumor-secreted Pros1 inhibits macrophage M1 polarization to reduce antitumor immune response. J Clin Invest. 2018;128(6):2356-69. doi: 10.1172/JCI97354.

37. Brown JM, Thomas R, Nagpal S, Recht L. Macrophage exclusion after radiation therapy (MERT): A new and effective way to increase the therapeutic ratio of radiotherapy. Radiother Oncol. 2020;144:159-64. doi: 10.1016/j.radonc.2019.11.020.

38. Yang Q, Guo N, Zhou Y, Chen J, Wei Q, Han M. The role of tumor-associated macrophages (TAMs) in tumor progression and relevant advance in targeted therapy. Acta Pharm Sin B. 2020;10(11):2156-70. doi: 10.1016/j.apsb.2020.04.004.

39. Zhao T, Wei T, Guo J, Wang Y, Shi X, Guo S, et al. PD-1-siRNA delivered by attenuated Salmonella enhances the antimelanoma effect of pimozide. Cell Death Dis. 2019;10(3):164. doi: 10.1038/s41419-019-1418-3.

Figure legends

Figure 1 with 1 supplement. The effect of radiotherapy in combination with nifuroxazide on the proliferation, migration and apoptosis of Hep G2 cells. (A) The effect of the radiotherapy in combination with nifuroxazide on the viability of Hep G2 cells by CCK-8 assay. (B) The effect of the radiotherapy in combination with nifuroxazide on the proliferation of Hep G2 cells by cell clone formation assay. (C) The effect of the radiotherapy in combination with nifuroxazide on the migration of Hep G2 cells by Wound-Healing assay. (D) The effect of the radiotherapy in combination with nifuroxazide on the migration of Hep G2 cells by transwell assay. (E) The effect of the radiotherapy in combination with nifuroxazide on the apoptosis of Hep G2 cells by flow cytometry assay. One-way ANOVA was carried out and the data were presented as mean ± SD (n=3). Compared with the control group, *P<0.05; compared with "4Gy" group, #P<0.05.

Figure 2. The effect of radiotherapy in combination with nifuroxazide on the expressions of tumor-associated proteins in cells. After radiotherapy, Hep G2 cells were treated with nifuroxazide at the different dose. At 24 h or 48 h after being incubated, the expression of tumor-associated proteins was detected by Western blot. (A-E) The expression of Stat3, p-Stat3, PCNA, Ki67 and cyclin D1 related with cell proliferation was analyzed by Western blot. (F-N) The expression of cytochrome C, pro-caspase 3, c-caspase 3, pro-caspase 9, c-caspase 9, Bax, Bcl-2, PARP and c-PARP related with cell apoptosis was analyzed by Western blot. One-way ANOVA was carried out and the data are presented as mean ± SD (n=3). Compared with the control group, *P<0.05; compared with "4Gy" group, #P<0.05.

Figure 3. The effects of radiotherapy in combination with nifuroxazide on tumor growth and survival of tumor-bearing mice. At 7 days after establishing the tumor model, the mice are received distinct treatments. (A) Treatment scheme of different methods. (B) Tumor pictures and tumor weight of tumor-bearing mice under different treatments are measured for statistical analysis. (C) The tumor volume changes of tumor-bearing mice under different treatments. (D) The survival of tumor bearing mice under different treatments. (E) Pathological pictures of tumor-bearing mice under different treatments. The ruler in the top row of the images represents 200 nanometers; the ruler in the bottom row of the images represents 50 nanometers. (F) Statistical analysis of pathological score. One-way ANOVA was carried out and the data are presented as mean ± SD (n=3) except Figure 3D, which was analyzed by Kaplan-Meier method. Compared with the PBS group, *P<0.05; compared with the

radiotherapy group, $*P*<0.05; compared with nifuroxazide group, #*P*<0.05.

Figure 4. The effects of radiotherapy in combination with nifuroxazide on the cell proliferation or apoptosis in tumor tissues. (A-C) The expression of Ki6, PCNA or c-caspase-3 in tumor tissues is detected by immunohistochemistry. The ruler in the top row of the images represents 200 nanometers; the ruler in the bottom row of the images represents 50 nanometers. (D) The cell apoptosis on tumor tissues is detected by TUNEL assay. (E-N) The protein expression of Stat3, p-Stat3, Ki67, PCNA, cyclin D1, cytochrome C, Bcl-2, Bax, pro-caspase 3 and c-caspase 3 in tumor tissues is detected by Western blot. One-way ANOVA was carried out and the data are presented as mean ± SD (n=3). Compared with the PBS group, *P<0.05; compared with the radiotherapy group, #P<0.05; compared with the nifuroxazide group, $$P$<0.05.

Figure 5. The effects of radiotherapy in combination with nifuroxazide on the infiltration of immune cells in tumor tissues. (A-C) Different isoforms of T lymphocytes infiltration in tumor tissues detected by immunofluorescence assay. (D) M1 macrophage infiltration in tumor tissues detected by immunofluorescence assay. (E) Statistical analysis about Semi quantitative of Figure A-D. (F-I) The protein expression of CD4, CD8, CD86 and Granzyme in tumor tissues is detected by Western blot. One-way ANOVA was carried out and the data are presented as mean ± SD (n=3). Compared with the PBS group, *P<0.05; compared with the radiotherapy group, #P<0.05; compared with the nifuroxazide group, $$P$<0.05.

Figure 6. The effect of radiotherapy in combination with nifuroxazide on the ratios of immune cells in spleens. The ratios of immune cells in the spleens of tumor-bearing mice were detected by flow cytometry. One-way ANOVA was carried out and the data are presented as mean ± SD (n=3). Compared with the PBS group, *P<0.05; compared with the radiotherapy group, #P<0.05; compared with the nifuroxazide group, $$P$<0.05.

Figure 7. Nifuroxazide in combination with the radiotherapy significantly increase the degradation of pd-l1 through ubiquitination proteasome pathway. (A) The expression of PD-L1 in cells combined treatment with radiotherapy and nifuroxazide is detected by Western blot. (B) The mRNA level of PD-L1 in cells is detected by PCR. (C-E) The effect of the radiotherapy combined with nifuroxazide on PD-L1 degradation through ubiquitination-proteasome pathway. (F) The schematic diagram of the mechanism that nifuroxazide degraded PD-L1 through ubiquitination-proteasome pathway. One-way ANOVA was carried out and the data are presented as mean ± SD (n=3). Compared with “0” group,

*P<0.05; compared with "4Gy" group, #P<0.05.

Figure 8. The effect of radiotherapy in combination with nifuroxazide on the expression of PD-L1 in tumor tissues. (A) PD-L1 expression in tumor tissues of HCC patients treated with radiotherapy are detected by immunofluorescence. (B) PD-L1 expression in tumor tissues of mice combined treatment with radiotherapy and nifuroxazide is detected by immunofluorescence. (C-D) The expression of PD-L1 or GSK3β in tumor tissues of mice combined treatment with radiotherapy and nifuroxazide is detected by Western blot. One-way ANOVA was carried out and the data were expressed as mean ± SD (n=3). Compared with the before-radiotherapy samples, **** P<0.0001; compared with the PBS group, *P<0.05; compared with the radiotherapy group, #P<0.05; compared with the nifuroxazide group, $$P$<0.05.

Figure 9. The synergistic antitumor mechanism of radiotherapy in combination with nifuroxazide in tumor-bearing mice. NK cell: natural killer cell. Treg: regulatory T cells. TAM: tumor-associated macrophage. $CD8^+$ CTL: $CD8^+$ cytotoxic lymphocyte.

Figure 1-figure supplement 1. The effect of radiotherapy and nifuroxazide on the proliferation, migration, and apoptosis of HepG2 cells. (A) The detection of radiotherapy combined with nifuroxazide on the viability of HepG2 cells using the CCK-8 assays. (B) The effect of radiotherapy and nifuroxazide on the migration of HepG2 through wound healing assays. (C) The influence of radiotherapy and nifuroxazide on the apoptosis of HepG2 cells using apoptosis assays.

Figure 5-figure supplement 2. The effect of combined nifuroxazide with radiotherapy on the immunocyte in tumor tissue of tumor-bearing mice. (A) The proportion of $CD4^+$ T lymphocytes in the tumor tissue of tumor-bearing mice after combination treatment. (B) The percentage of $CD8^+$ T lymphocytes in the tumor tissue of tumor-bearing mice after combination treatment. (C) The proportion of $Tregs^+$ T lymphocytes in the tumor tissue of tumor-bearing mice after combination treatment. (D) The percentage of Granzyme B^+ lymphocytes in the tumor tissue of tumor-bearing mice after combination treatment. (E) The ratio of NK cells in the tumor tissue of tumor-bearing mice after combination treatment.

Figure 7-figure supplement 3. The effect of nifuroxazide on PD-L1 expression in Huh7 cells. (A)

The effect of the combination therapy using nifuroxazide and radiotherapy on the expression of PD-L1 protein in Huh7 cells using Western blot analysis. (B) The effect of combined nifuroxazide with radiotherapy on the expression of PD-L1 gene in Huh7 cells via qPCR. (C) The effect of proteasome inhibitor MG132 on the expression of PD-L1.

Figure 1

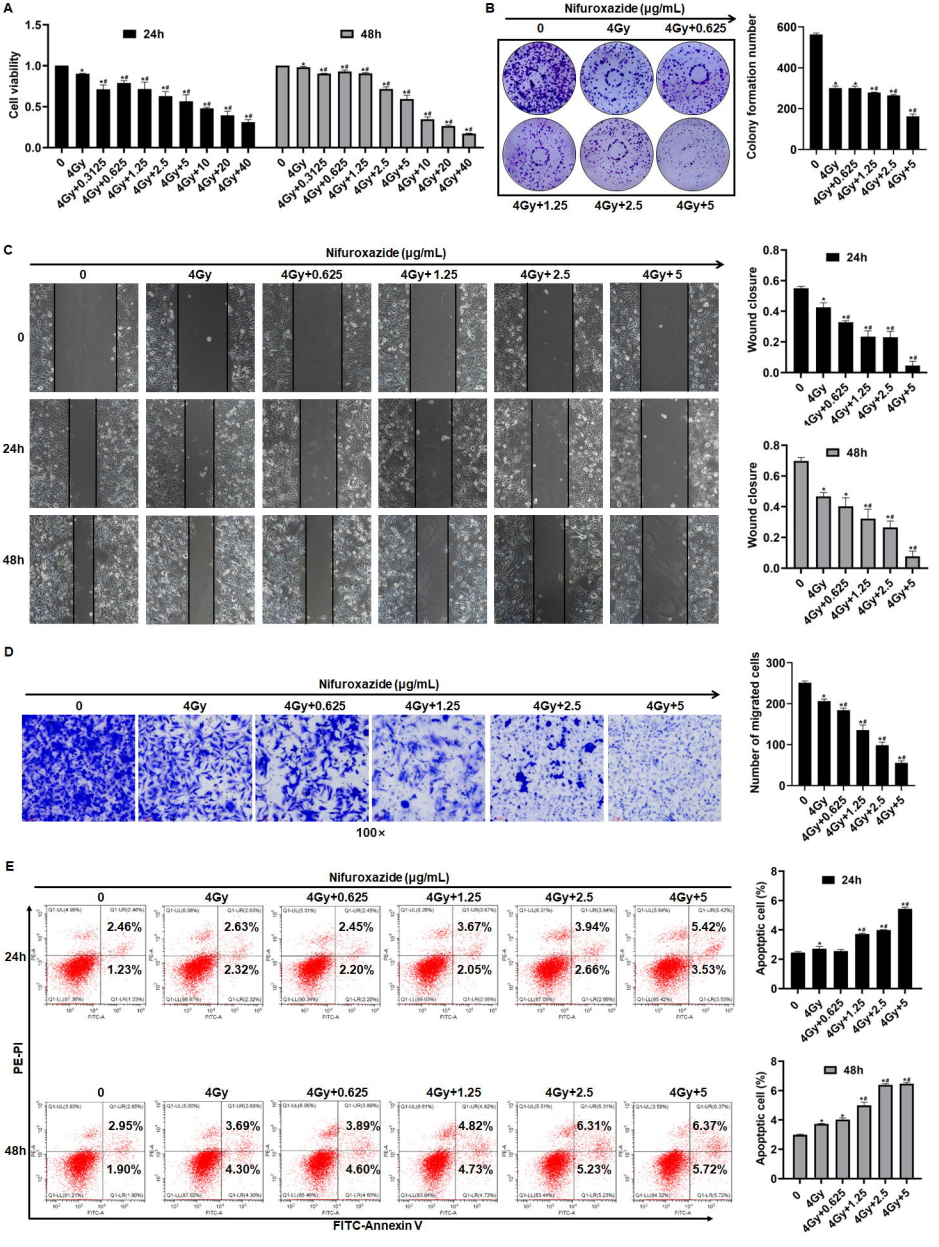
A
24h
48h
Cell viability
0
4Gy
4Gy+0.3125
4Gy+0.625
4Gy+1.25
4Gy+2.5
4Gy+5
4Gy+10
4Gy+20
4Gy+40
B
Nifuroxazide (μg/mL)
0
4Gy
4Gy+0.625
4Gy+1.25
4Gy+2.5
4Gy+5
Colony formation number
C
Nifuroxazide (μg/mL)
0
4Gy
4Gy+0.625
4Gy+1.25
4Gy+2.5
4Gy+5
24h
48h
Wound closure
D
Nifuroxazide (μg/mL)
0
4Gy
4Gy+0.625
4Gy+1.25
4Gy+2.5
4Gy+5
100×
Number of migrated cells
E
Nifuroxazide (μg/mL)
0
4Gy
4Gy+0.625
4Gy+1.25
4Gy+2.5
4Gy+5
24h
48h
PE-PI
FITC-Annexin V
Apoptptic cell (%)

Figure 2

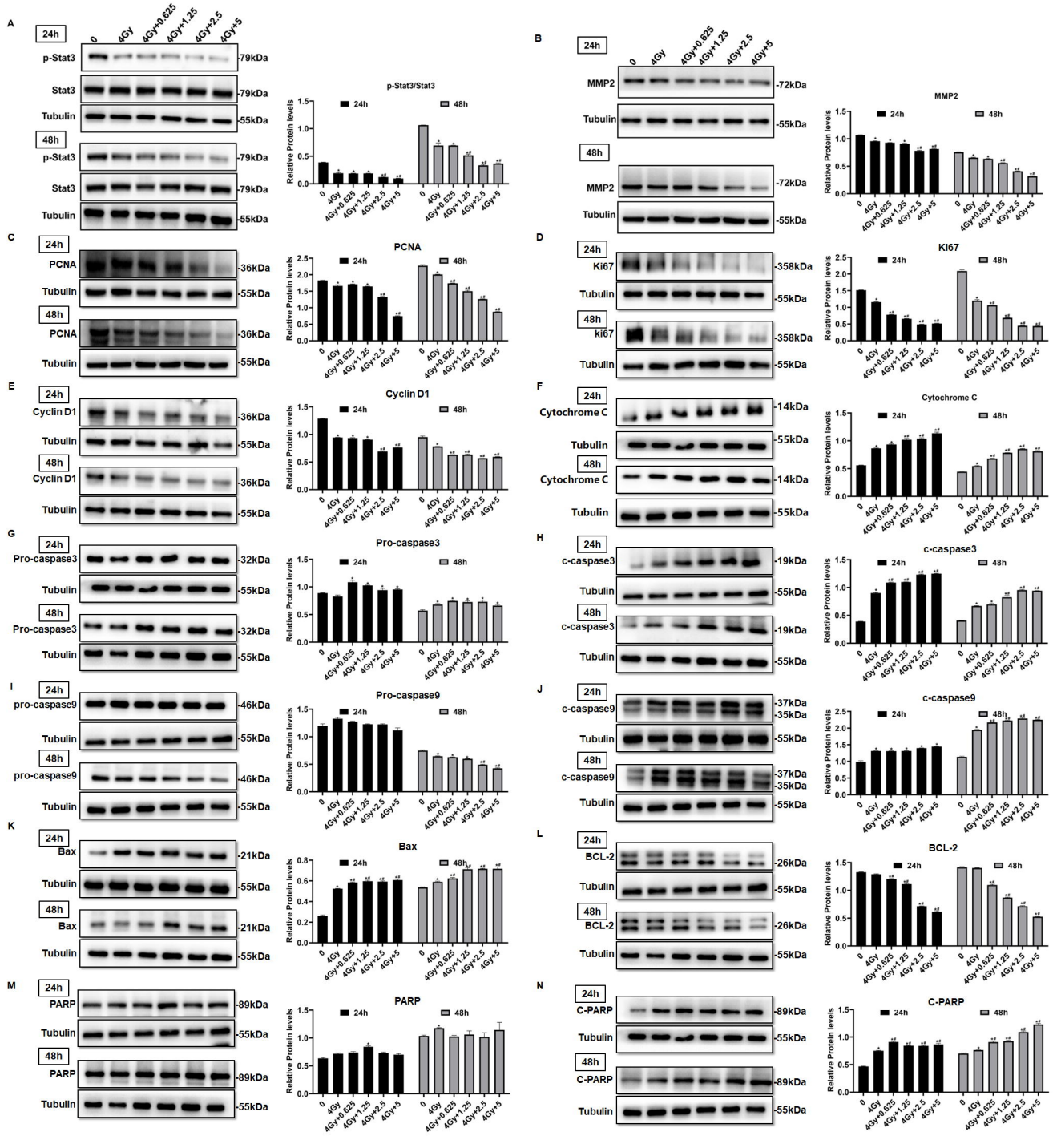
A
24h
0
4Gy
4Gy+0.625
4Gy+1.25
4Gy+2.5
4Gy+5
p-Stat3
79kDa
Stat3
79kDa
Tubulin
55kDa
48h
p-Stat3
79kDa
Stat3
79kDa
Tubulin
55kDa
p-Stat3/Stat3
24h
48h
Relative Protein levels
B
MMP2
72kDa
MMP2
C
PCNA
36kDa
PCNA
D
Ki67
358kDa
Ki67
E
Cyclin D1
36kDa
Cyclin D1
F
Cytochrome C
14kDa
Cytochrome C
G
Pro-caspase3
32kDa
Pro-caspase3
H
c-caspase3
19kDa
c-caspase3
I
pro-caspase9
46kDa
Pro-caspase9
J
c-caspase9
37kDa
35kDa
c-caspase9
K
Bax
21kDa
Bax
L
BCL-2
26kDa
BCL-2
M
PARP
89kDa
PARP
N
C-PARP
89kDa
C-PARP

Figure 3

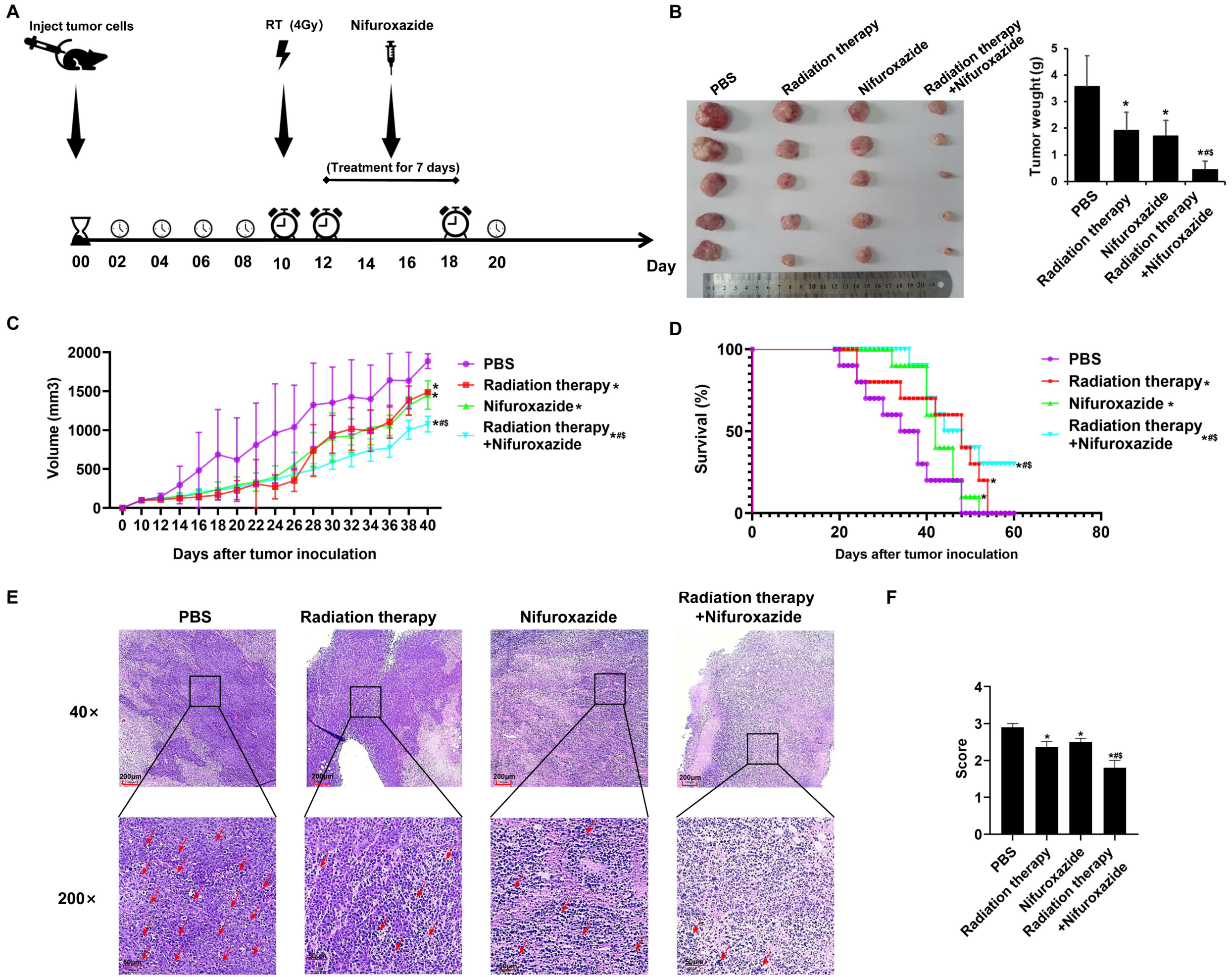
A
Inject tumor cells
RT (4Gy)
Nifuroxazide
(Treatment for 7 days)
00 02 04 06 08 10 12 14 16 18 20
Day
B
PBS
Radiation therapy
Nifuroxazide
Radiation therapy +Nifuroxazide
Tumor weught (g)
C
Volume (mm3)
Days after tumor inoculation
PBS
Radiation therapy
Nifuroxazide
Radiation therapy +Nifuroxazide
D
Survival (%)
Days after tumor inoculation
E
PBS
Radiation therapy
Nifuroxazide
Radiation therapy +Nifuroxazide
40×
200×
F
Score

Figure 4

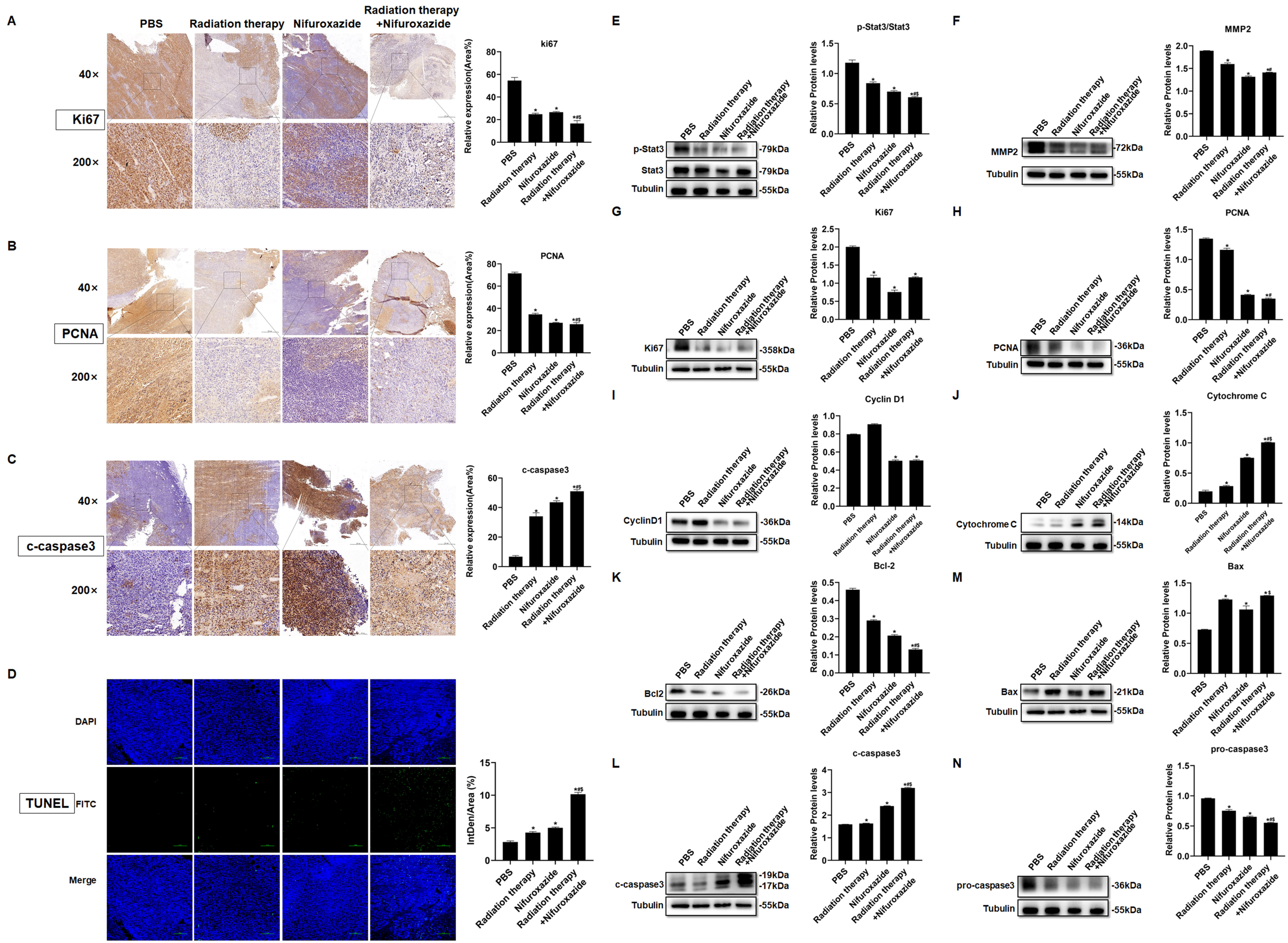
A
PBS
Radiation therapy
Nifuroxazide
Radiation therapy +Nifuroxazide
40×
Ki67
200×
ki67
Relative expression(Area%)
B
PCNA
c-caspase3
C
DAPI
TUNEL
FITC
Merge
IntDen/Area (%)
E
p-Stat3/Stat3
p-Stat3
Stat3
Tubulin
-79kDa
-55kDa
Relative Protein levels
F
MMP2
-72kDa
G
Ki67
-358kDa
H
PCNA
-36kDa
I
Cyclin D1
CyclinD1
J
Cytochrome C
-14kDa
K
Bcl-2
Bcl2
-26kDa
M
Bax
-21kDa
L
c-caspase3
-19kDa
-17kDa
N
pro-caspase3
PBS
Radiation therapy
Nifuroxazide
Radiation therapy +Nifuroxazide

Figure 5

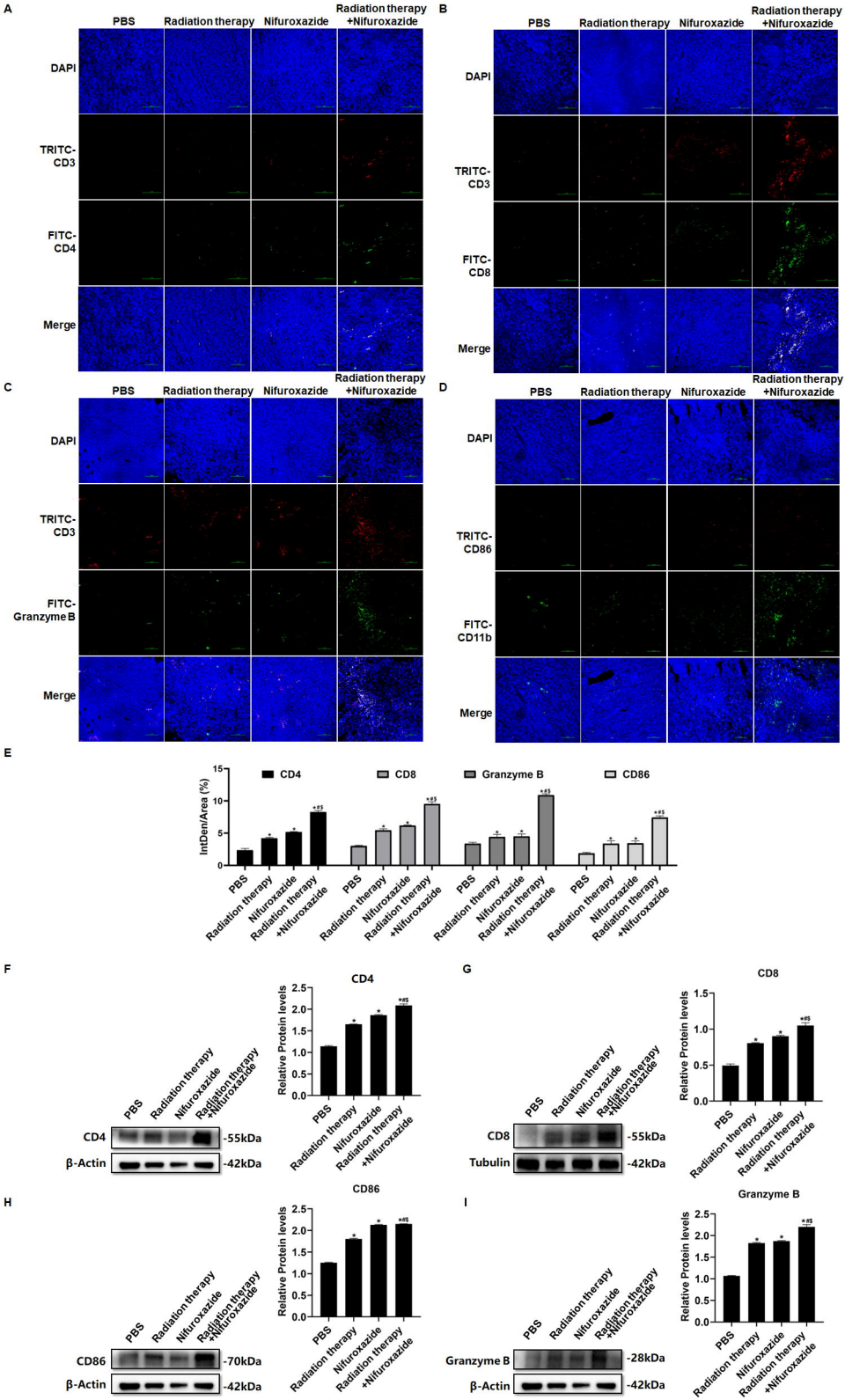
A
PBS
Radiation therapy
Nifuroxazide
Radiation therapy +Nifuroxazide
DAPI
TRITC-CD3
FITC-CD4
Merge
B
DAPI
TRITC-CD3
FITC-CD8
Merge
C
DAPI
TRITC-CD3
FITC-Granzyme B
Merge
D
DAPI
TRITC-CD86
FITC-CD11b
Merge
E
CD4
CD8
Granzyme B
CD86
IntDen/Area (%)
F
CD4
Relative Protein levels
CD4
β-Actin
-55kDa
-42kDa
G
CD8
Tubulin
-55kDa
-42kDa
H
CD86
CD86
β-Actin
-70kDa
-42kDa
I
Granzyme B
Granzyme B
β-Actin
-28kDa
-42kDa

Figure 6

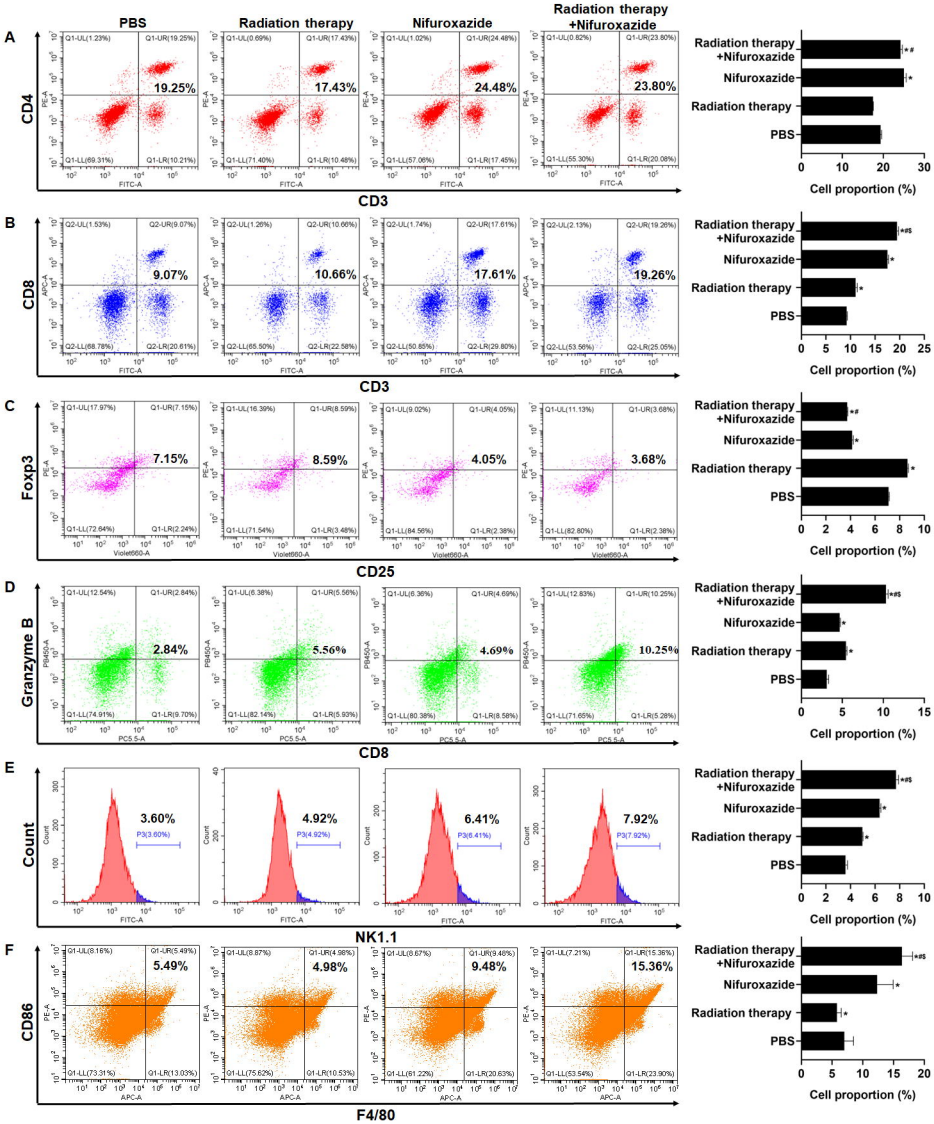
PBS
Radiation therapy
Nifuroxazide
Radiation therapy +Nifuroxazide
A
CD4
CD3
19.25%
17.43%
24.48%
23.80%
B
CD8
CD3
9.07%
10.66%
17.61%
19.26%
C
Foxp3
CD25
7.15%
8.59%
4.05%
3.68%
D
Granzyme B
CD8
2.84%
5.56%
4.69%
10.25%
E
Count
NK1.1
3.60%
4.92%
6.41%
7.92%
F
CD86
F4/80
5.49%
4.98%
9.48%
15.36%
Radiation therapy +Nifuroxazide
Nifuroxazide
Radiation therapy
PBS
Cell proportion (%)

Figure 7

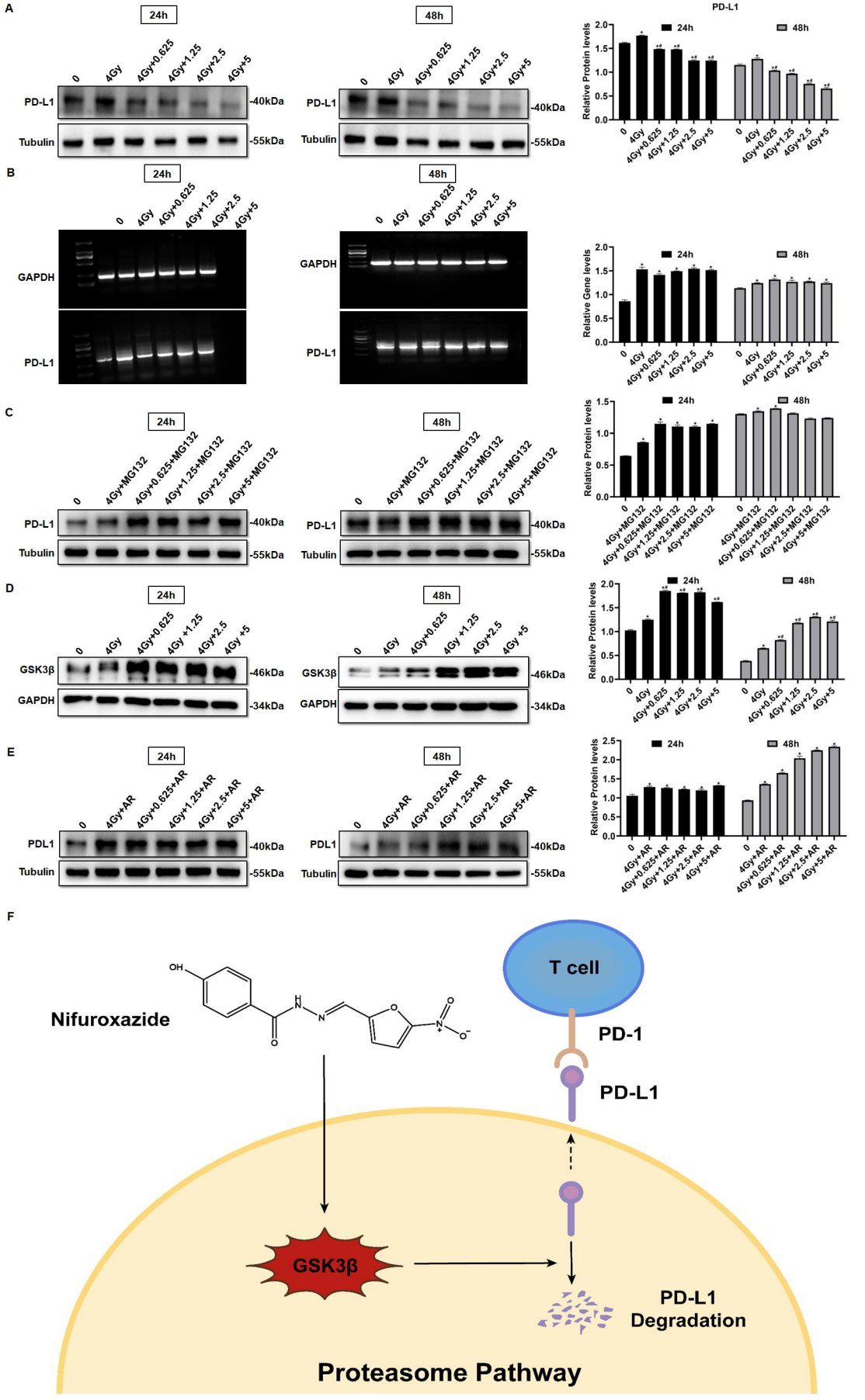
A
24h
48h
0
4Gy
4Gy+0.625
4Gy+1.25
4Gy+2.5
4Gy+5
PD-L1
Tubulin
40kDa
55kDa
PD-L1
Relative Protein levels
B
GAPDH
PD-L1
Relative Gene levels
C
4Gy+MG132
4Gy+0.625+MG132
4Gy+1.25+MG132
4Gy+2.5+MG132
4Gy+5+MG132
D
GSK3β
GAPDH
46kDa
34kDa
E
4Gy+AR
4Gy+0.625+AR
4Gy+1.25+AR
4Gy+2.5+AR
4Gy+5+AR
PDL1
F
Nifuroxazide
T cell
PD-1
PD-L1
GSK3β
PD-L1
Degradation
Proteasome Pathway

Figure 8

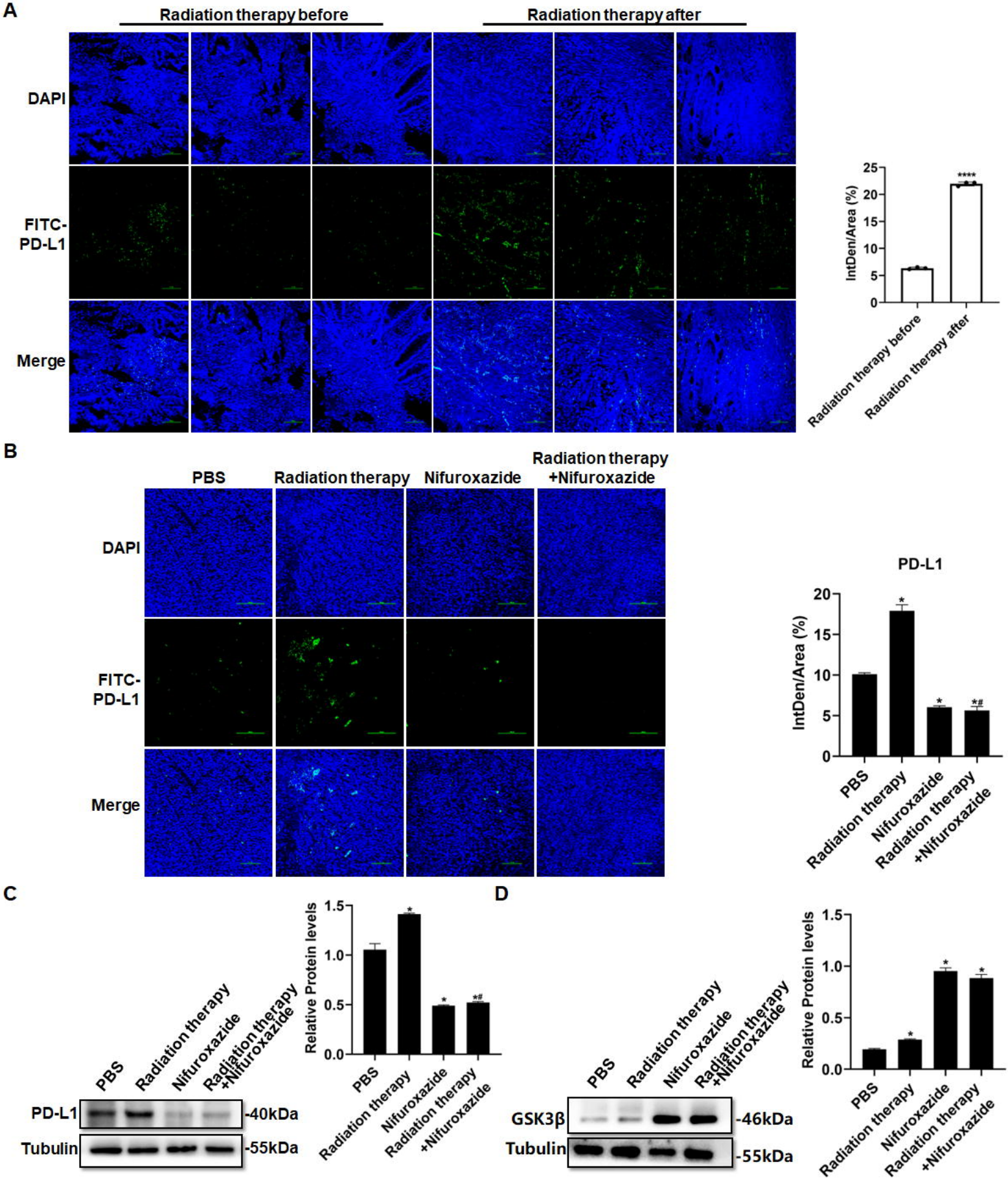
A
Radiation therapy before
Radiation therapy after
DAPI
FITC-PD-L1
Merge
IntDen/Area (%)
****
Radiation therapy before
Radiation therapy after
B
PBS
Radiation therapy
Nifuroxazide
Radiation therapy +Nifuroxazide
DAPI
FITC-PD-L1
Merge
PD-L1
IntDen/Area (%)
PBS
Radiation therapy
Nifuroxazide
Radiation therapy +Nifuroxazide
C
PBS
Radiation therapy
Nifuroxazide
Radiation therapy +Nifuroxazide
PD-L1
-40kDa
Tubulin
-55kDa
Relative Protein levels
D
PBS
Radiation therapy
Nifuroxazide
Radiation therapy +Nifuroxazide
GSK3β
-46kDa
Tubulin
-55kDa
Relative Protein levels

Figure 9

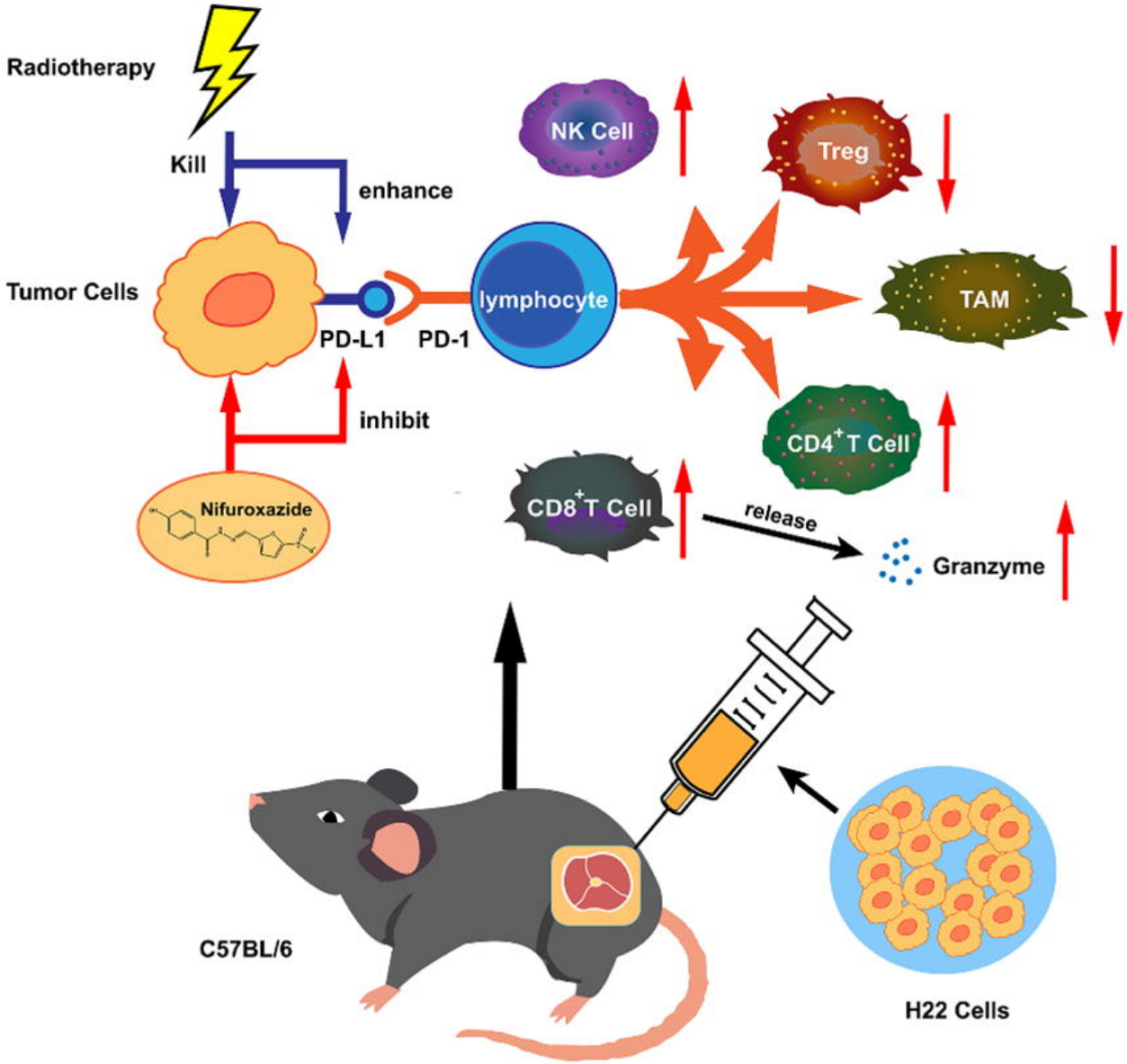
Radiotherapy
Kill
enhance
Tumor Cells
PD-L1
PD-1
lymphocyte
NK Cell
Treg
TAM
CD4+ T Cell
CD8+ T Cell
release
Granzyme
inhibit
Nifuroxazide
C57BL/6
H22 Cells